Available online at www.sciencedirect.com
SCIENCE DIRECT®
Microporous and Mesoporous Materials 86 (2005) 249–255
MICROPOROUS AND MESOPOROUS MATERIALS
www.elsevier.com/locate/micromeso

Comparative study of natural and synthetic clinoptilolites containing silver in different states

B. Concepción-Rosabal [a,*], G. Rodríguez-Fuentes [a], N. Bogdanchikova [b], P. Bosch [c], M. Avalos [b], V.H. Lara [d]

[a] *Laboratorio de Ingeniería de Zeolitas, IMRE-Facultad de Física, Universidad de La Habana, C.P 10400 La Habana, Cuba*
[b] *CCMC, UNAM, Ensenada, Apdo Postal 2681, B.C. 22800 México, Mexico*
[c] *Instituto de Investigaciones en Materiales, UNAM, Ciudad Universitaria, Apdo Postal 70360, 04510 México DF, Mexico*
[d] *Universidad Autónoma Metropolitana-Iztapalapa, Michoacán y La Purísima, 09340 México DF, Mexico*

Received 13 April 2004; received in revised form 19 July 2005; accepted 20 July 2005
Available online 12 September 2005

Abstract

Clinoptilolite is a widely used natural zeolite due to its abundance in nature. The present work discusses the characteristics of silver modified clinoptilolites (natural and synthetic) containing silver in different states. The results obtained by the combined use of XRD, UV–Visible spectroscopy, and SAXS are described. These analyses were carried out to determine the features of silver in the zeolitic structure (natural and synthetic) and the particle size distribution of the Ag conglomerates produced in the reduced samples.

The crystalline structure of the Ag-synthetic clinoptilolite was not affected by the thermal reduction of Ag; however, the Ag-natural clinoptilolite samples were less thermally stable. In synthetic and natural clinoptilolites after reduction at 100 °C, small clusters (radius of <0.5 nm) located inside the channels along with metal particles (with radius <7 nm) on the external surface were observed. In Ag-natural clinoptilolite reduced at 100 °C, along with the small Ag_2^+ and $Ag_4^{\delta+}$ clusters stabilized inside clinoptilolite pores, large Ag_8^0 and $Ag_8^{\delta+}$ clusters can be formed inside large mordenite channels or in the interstitial spaces of the particles that compose this mineral. Reduction at 400 °C leads to disappearance of silver clusters and large particle formation. In both supports the particles cannot be located in the zeolite cavities, which are much smaller.

Keywords: Zeolites; Clinoptilolite; Cation exchange; Silver clusters

1. Introduction

Zeolites are natural and synthetic hydrated crystalline aluminosilicates with adsorptive and ion exchange properties. Heulandite and the isostructural clinoptilolite (IUPAC code HEU, [1]) are widely used natural zeolites, due to their selective cation-exchange properties and to their widespread availability [2]. New materials with a great variety of physical–chemical properties resulting from modifications (mainly ion exchange) of natural clinoptilolite have been thoroughly studied in the last years in numerous experimental and theoretical works [3–12].

Clinoptilolite crystallizes in monoclinic *C2/m* group with the following unit cell parameters: $a = 17.62$ Å, $b = 17.91$ Å, $c = 7.39$ Å and $\beta = 116.40°$ [1]. The structure of clinoptilolite has a two-dimensional three channel system, occupied by cations and water, molecules: channel a and channel b running parallel to the [0 0 1] axis, formed by 10-membered ring and 8-membered ring, respectively, and channel c, running parallel

* Corresponding author. Tel.: +53 778 8957; fax: +53 779 4651.
E-mail address: beatriz@fisica.uh.cu (B. Concepción-Rosabal).

1387-1811/$ - see front matter © 2005 Elsevier Inc. All rights reserved.
doi:10.1016/j.micromeso.2005.07.027

to [1 0 0] and [1 0 2], formed by 8-membered ring. In this two-dimensional channel system, two cages are formed due to the intersections between the channels: cage I, intersection of channel c with channel a, and cage II, intersection of channel c with channel b.

The clinoptilolite has four cationic sites (M1, M2, M3 and M4) where ion exchange occurs. The theoretical composition of this zeolite is $(K_2, Na_2, Ca)_3[Al_6Si_{30}O_{72}]\cdot 24H_2O$, it can also contain some Mg^{2+} and Fe^{2+} ions [13]. The content of non-tetrahedral cations (K^+, Na^+, Ca^{2+}) as well as Si/Al ratio can change depending on the mineral. Fig. 1 shows the structure of clinoptilolite through *c*-axis and the preferential sites occupied by the natural cations according to Koyama and Takeushi [14].

An interesting advance in zeolite technology has been the development of novel antimicrobial agents based on synthetic and natural zeolites [15–18]. Among them, compounds containing silver are attractive because of their strong antibacterial activity, high stability, and wide antibacterial spectrum [19,20]. For the preparation of such materials, zeolite has been used as carrier and slow releaser of the silver ions with olygodynamic properties. The oxidation state of the exchanged metal and the possibility to release it slowly and continually could determine the microbicide effectiveness.

Since the characteristics of antibacterial Ag-zeolites significantly depend of the different forms of occluded silver, it would be useful to study the influence of different silver species supported on zeolites as for the antibacterial activity. Recently, in a previous work, Bogdanchicova et al. [21] carried out extensive experiments to investigate antibacterial and antiviral activities of Cuban natural clinoptilolite (source material) and its silver modified forms against *Escherichia coli* (TAR90) and *Phagocyte lambda* (DASH II Stratagene). Change

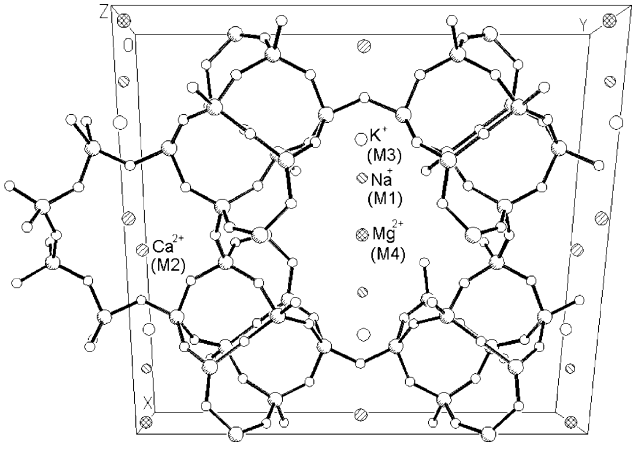

Fig. 1. Structure of clinoptilolite through *c*-axis and the preferential sites that occupy the natural cations according to reported by Koyama and Takeushi [14].

of the reduction temperature from 20 to 600 °C permitted to prepare Ag-natural clinoptilolite samples with varying contribution of the different states of silver. Small silver clusters, Ag_n subcolloidal particles ($n = 10$), and large silver particles are formed on zeolite surface. Stability of Ag-natural clinoptilolite samples during storage in air was found to be very high. The microbiologic studies demonstrated that the samples with silver cationic and cluster species possess the high antibacterial and antiviral activity. The well documented facts that this Cuban natural zeolite is innocuous to the human being and its demonstrated stability during the transit through the gastrointestinal tract [4,22], as well as the natural abundance of the raw material, are essential elements when considering the different Ag-natural clinoptilolite composites as an antibacterial material of potential pharmaceutical use.

Similar to the conditions as referred above, during the hydrogen reduction of Ag-natural and synthetic clinoptilolites formation of different silver, reduced species is observed. The modifications performed on the zeolites allow controlling re-oxidation processes of these clusters and colloidal particles. The oxidation of clusters and colloidal particles lead to the reversible formation of Ag^+ ions, which can be released to media in the usual way for zeolites through mechanism of ion exchange. The differences in each case allow the creation of sources of ions for release, with a possibility to accelerate or decelerate ions formation velocity. It is desirable to have a system that can gradually release Ag^+ and, therefore, increase the liberation period of the substrate.

Clinoptilolite was chosen as it is present in Mexico (Oaxaca deposits), as well as in Cuba (Tasajeras deposits). As the amount of silver content is a critical parameter in the performance of such exchanged materials, the present work discusses a silver modified natural clinoptilolite compared to the corresponding synthetic clinoptilolite. Natural zeolites may vary in composition and morphology from one deposit to another, because they are extracted mainly from volcanic and sedimentary rocks with other zeolitic and non-zeolitic mineral phases, which are difficult to remove [23]. A sample of natural zeolite with 100% purity is, indeed, a geological museum masterpiece. Therefore, we compare the features of a natural zeolite exchanged with silver to the corresponding synthetic zeolite. We are, indeed, interested to determine how much such compositional variations could affect silver exchange.

States of silver stabilized in synthetic mordenites were intensively and systematically investigated [24–26]. But we could not find publications dedicated to forms of silver stabilized in pure clinoptilolites in the literature. Knowledge of silver state in clinoptilolite planned to obtain in this work in combination with data on silver states in mordenite [25] will allow selecting natural zeolite stabilizing silver in states desirable for commercial

Ag-natural zeolites applied for water purification and medicine.

In this paper, the results obtained by the combined use of X-ray diffraction (XRD), UV–visible diffuse reflectance spectroscopy (DRS), and small angle X-ray scattering (SAXS) are described. These analyses were carried out to determine the state of silver in the zeolitic structure and to study the particle size distribution of the Ag agglomerates produced in the reduced samples.

2. Experimental

The natural clinoptilolite (NC) is the purified zeolite material, obtained from the zeolitic rock of the Tasajeras deposit (Cuba). NC is a mixture of about 78% clinoptilolite–heulandite and 5% of mordenite and 17% of other mineral phases (quartz, feldspar, montmorillonite and iron oxides). The oxide form chemical composition of NC was found to be [6] (with the balance as H_2O): 66.5 (SiO_2), 11.3 (Al_2O_3), 4.3 (CaO), 2.0 (Na_2O), 0.6 (K_2O), 0.5 (MgO), 1.1 (Fe_2O_3). This natural zeolite does not cause any biological damage in humans as shown by toxicological tests [22]. Synthetic Na, K-clinoptilolite-100% purity-(SC) was prepared and supplied by Dr. A. Prakash, Department of Chemistry, University of Houston, Houston, USA.

Ag-clinoptilolite samples (natural and synthetic) were prepared by ion exchange using an $AgNO_3$ solution as was described elsewhere [27].[1] Natural clinoptilolite was previously transformed into sodium form to increase the efficiency of ionic exchange. The obtained samples were thoroughly washed with distilled water to remove the excess salt and finally dried at 60 °C. Ag-clinoptilolite samples were reduced in a hydrogen flow for 2.5 h at different reduction temperatures (100–600 °C), employed a temperature ramp rate of 10 °C/min. Silver containing natural and synthetic clinoptilolite samples were designed as Ag-NC and Ag-SC, respectively, followed by the value of the reduction temperature (°C). For example, Ag-NC100 means silver containing natural clinoptilolite reduced at 100 °C.

The amount of silver in the samples, Ag-NC and Ag-SC, was determined by energy disperse spectroscopy (EDS), with a Kevex superdry detector and the MAGIC V program supplied by Kevex were applied.

UV–vis diffuse reflectance spectra (UV–vis DRS) registered just after sample reduction and during sample storage in air were recorded under ambient conditions on a CARY SCAN 300 (VARIAN) with standard diffuse reflectance unit. Reference samples were the natural (Na-form) and synthetic clinoptilolite matrices treated in hydrogen under the same conditions as Ag containing samples. Measurements were made in the wavelength range of 190–850 nm. UV–vis spectra presented in the article were obtained by subtracting spectrum of reference sample from the spectrum of studied sample.

The crystalline compounds were identified by X-ray diffraction with a Philips X'pert diffractometer. CuKα ($\lambda = 0.154$ nm) radiation was selected with a curved graphite monochromator. All X-ray diffraction patterns were recorded under ambient conditions in the angular interval of $5° < 2\theta < 60°$.

To determine the size and shape of silver clusters and particles small angle X-ray scattering (SAXS) was used. CuKα radiation was selected with a Ni filter and the intensity curve was recorded with a Kratky camera coupled to a linear proportional counter. Intensity $I(h)$ was measured for 9 min in order to obtain good quality statistics. The SAXS data were processed with the ITP program [28–31]. The angular parameter (h) is defined as $h = (4\pi \sin\theta/\lambda)$, where 2θ and λ are X-ray scattering angle and wavelength, respectively. The radius of gyration, R_g, could then be obtained from the slope of the Guinier plot: $\mathrm{Log}\, I(h)$ vs h^2 [32]. Before SAXS measurements, the powdered samples were evacuated to eliminate adsorbed water.

The globular or fibrous shape of the sample was estimated from the Kratky plot, i.e., $h^2 I(h)$ vs h [33,34]. Assuming a shape [35], the distance distribution functions, i.e. the size distribution of the scattering objects, may be calculated. It is often useful to estimate from the slope of the curve $\mathrm{Log}\, I(h)$ vs. $\mathrm{Log}\, h$ the fractal dimension of the scattering objects [36,37] to define the degree of roughness or the degree of connectivity of the scattering objects. For this study, the background obtained with the Porod plot was subtracted from the experimental intensity.

3. Results and discussion

The chemical analysis of silver containing samples indicates that the synthetic clinoptilolite Ag-SC has 3.90 wt.% (0.36 meq/g) of silver while Ag-NC has 2.16 wt.% (0.20 meq/g). The difference in the uptake of Ag^+ cations during the exchange reaction is due to the differences in the chemical and phases composition of these samples. It is known that the Si/Al ratio determines the theoretical exchange capacity [38]. Synthetic clinoptilolite has a slightly smaller Si/Al ratio than natural clinoptilolite (Si/Al = 5 for SC and Si/Al = 5.3 for NC) thus, it is expected that the uptake of silver in this material will be larger. In addition, the presence of non-porous phases in natural clinoptilolite (about 17% of quartz, feldspar, montmorillonite and iron oxides) reduces its theoretical ion exchange capacity.

X-ray diffraction (XRD) experiments showed that the sample Na, K-clinoptilolite (synthetic) is only

[1] Cuban patent in progress.

clinoptilolite (JCPDS card 25-1349). If compared to the natural sample NC, the presence of other crystalline compounds is clearly revealed: mordenite, quartz and feldspar (anorthite). In Figs. 2 and 3 these results are shown.

The inspection of the XRD patterns confirms that no transition of zeolite phases occurs during Ag ion exchange. Variations in the relative intensities of the (020) and (200) clinoptilolite peaks were found in these XRD patterns after Ag ion exchange. These changes in peak intensity are mainly associated with differences in the nature, amount and position of the extra-framework species in clinoptilolite channels. It should be considered not only with the Ag^{+} ions, but also a remained amount of native cations in the clinoptilolite, which is common in ion exchange with both natural and synthetic zeolites [38]. According to Petrov [39] in a study of cation exchange in clinoptilolite, the intensity of the (020) peaks is the most likely to vary, since it is strongly related to the extra-framework species sited in the mirror plane perpendicular to the *b*-axis. Therefore, variations in the channel content mainly affect these peaks, leaving other peaks almost unaltered. We note that a similar behavior was observed when other Cuban natural clinoptilolites were treated with sodium carbonate, ammonium and iron solutions [6,8,40].

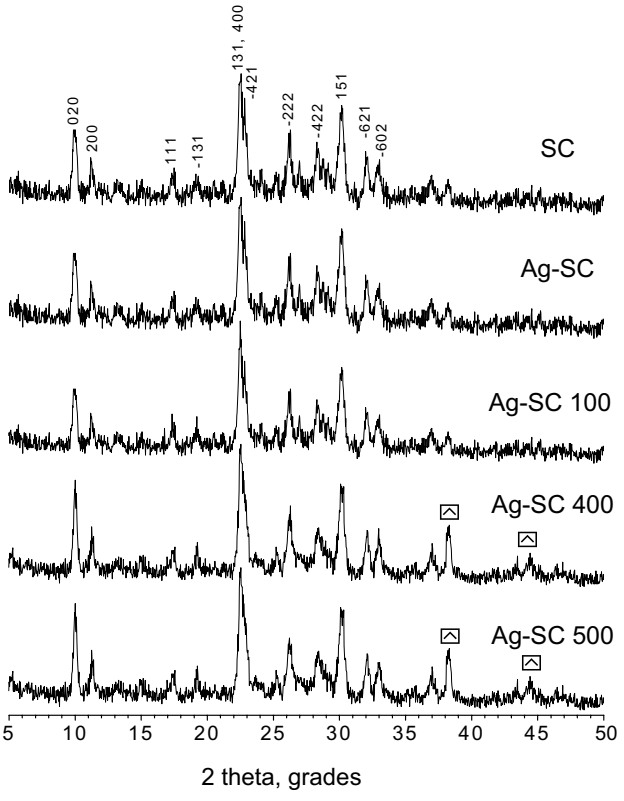

Fig. 2. X-ray powder patterns of synthetic clinoptilolite (SC), Ag-synthetic clinoptilolite (Ag-SC), and Ag-synthetic clinoptilolite reduced at different temperatures (Ag-SC100, Ag-SC400 and Ag-SC500). The Miller indexes of the main reflections for Na,K-clinoptilolite (synthetic) are shown. The △ indicates the peaks (111) and (200) corresponding to Ag, ICSD#64706.

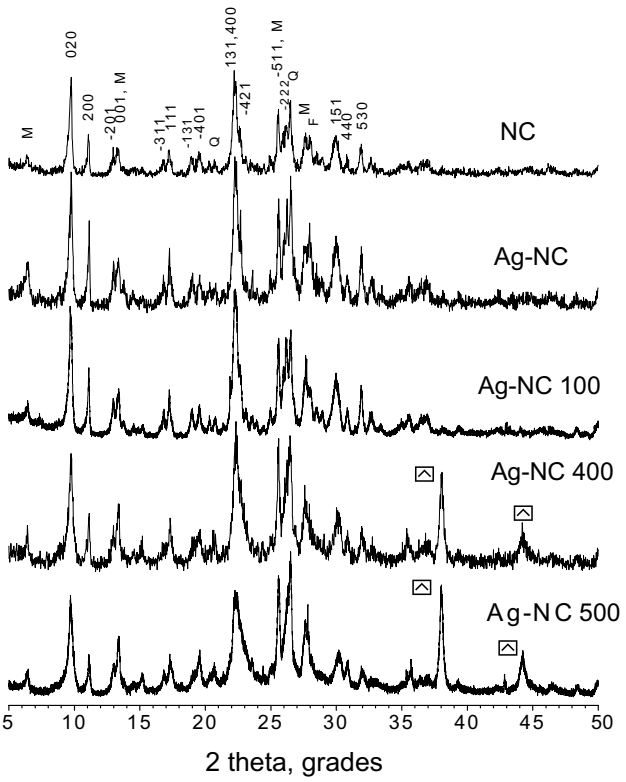

Fig. 3. X-ray powder patterns of natural clinoptilolite (NC), Ag-natural clinoptilolite (Ag-NC), and Ag-natural clinoptilolite reduced at different temperatures (Ag-NC100, Ag-NC400 and Ag-NC500). The Miller indexes of the main reflections for clinoptilolite–heulandite are shown. Others labeled reflections correspond to M = mordenite, Q = quartz, F = feldspar. The △ indicates the peaks (111) and (200) corresponding to Ag, ICSD#64706.

The reduction process provokes variations in relative intensities of the peaks of clinoptilolite (Figs. 2 and 3). It could be due to the appearance of silver clusters and quasi-colloidal particles in zeolite in both samples confirmed by UV–Visible spectroscopy results presented below.

The crystalline structure of Ag-SC was not affected by the thermal reduction process, however; the Ag-NC samples were lightly less thermally stable. A loss of crystallinity in Ag-NC was found when the reduction temperature was increased. At 500 °C, the deformation of the peaks characteristic for clinoptilolite is remarkable. The intensity of the (020), (131), (400) and (−421) diffraction maximum of Ag-NC500 decrease slightly and an increase of the background between 15° and 35° 2θ is evident.

It is well-known that the thermal behavior of clinoptilolite–heulandite zeolites is mainly dependent on the extra-framework cation contents of the zeolite and, to a certain extent, on its Si/Al ratio [41]. On the other hand, experimental works in natural and cation-ex-

changed clinoptilolite carried out by Langella et al. [42] allowed them to formulate the following sequence of thermal stability: $Cs^+ \cong K^+ > NH_4^+ > Na^+ > Sr^{2+} \cong Ca^{2+} \cong Mg^{2+} > Li^+$. In particular, the high content of K^+ cation stabilizes the crystalline structure up to 600 °C, whereas, at this temperature, thermal collapse of the zeolitic structure is almost complete for the other six cation forms.

On NC, (such it was reported in Section 2), Ca^{2+} is the major exchangeable cation followed by Na^+, K^+, Fe^{2+} and Mg^{2+}. The existence of different exchangeable cations on NC is the responsible of its less thermally stability compared to SC.

Peaks at 38.12° and 44.28°, characteristic of metallic Ag, may be attributed to the presence of large Ag particles after reduction of Ag-SC samples at 400 °C. In the XRD patterns of Ag-NC samples, the same peaks appear after reduction at 400 °C. Due to the large size of these particles, they can be located only outside of the clinoptilolite and mordenite channels. The above-mentioned was confirmed for SAXS results presented below.

In Fig. 4, UV–vis diffuse reflectance spectra of all studied reduced samples are presented. Interpretation of all observed peaks was accomplished as in Ref. [25]. Fig. 4(a) presents the UV–vis DR spectra of Ag-NC100 and Ag-SC100. Both samples have quasi-colloidal particles of Ag (size ~1 nm) formed at the external surface of clinoptilolite crystals as shown by the peak at 380 nm. The peaks observed at 276 and 310 nm in the spectrum of Ag-SC100 sample are attributed to clusters of $Ag_4^{\delta+}$ and Ag_2^+, respectively [25]. These peaks are observed as shoulders in the case of Ag-NC100. This fact suggest that only a small amount of $Ag_4^{\delta+}$ and Ag_2^+ clusters inside natural clinoptilolite pores are formed after reduction. Ag_2^+ clusters must be located in cage II formed (intersection of channel c with channel b). The remaining Ca^{2+} cations in M2 cationic position inhibit a numerous formation of Ag_2^+ clusters in Ag-NC100 sample.

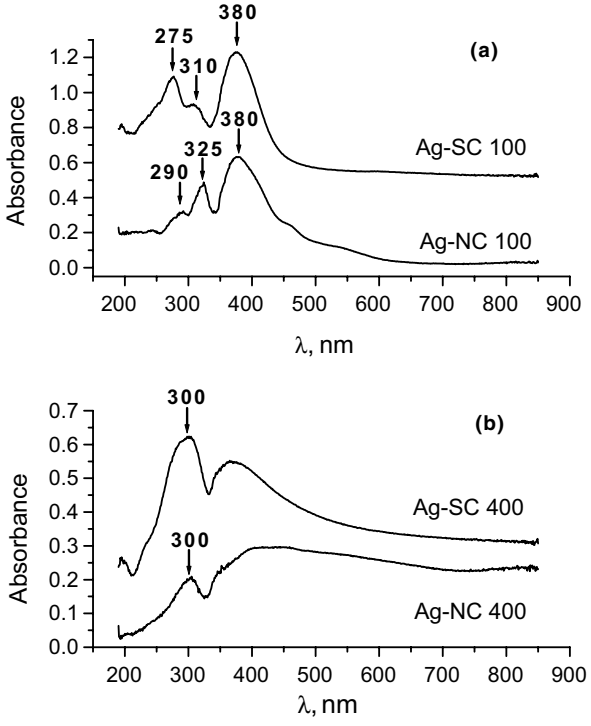

Fig. 4. Comparison of UV–vis diffuse reflectance spectra of Ag-natural clinoptilolite (Ag-NC) and Ag-synthetic clinoptilolite (Ag-SC) reduced at different temperatures. (a) Reduced at 100 °C, (b) reduced at 400 °C.

Clinoptilolite in natural environments may have several cations on the exchange sites, but the most common cations are Na^+, K^+ and Ca^{2+}. It is well-known that Clinoptilolite exhibits cation selectivity, e.g., Ca^{2+} is easily replaced with Na^+, but K^+ in the zeolite is replaced with difficulty by either Ca^{2+} or Na^+ [43]. Even if the samples were sodium-exchange, they contain Ca^{2+} ions as shown by Cappelletti et al. [44] who determined the cation exchange capacity of two representative clinoptilolite enriched samples (98% zeolite in both samples). The results revealed that only 70–80% Ca^{2+} and 60–70% of the Mg^{2+} was exchanged. On the other hand, synthetic clinoptilolite (SC) contains only Na^+ and K^+ cations. The Ag^+ exchange in SC leads to the release of the Na^+ cations present at M1 positions in cage-II because there were no Ca^{2+} cations in M2 position. Then, the location of two Ag^+ cations in M1 sites at cage-II produced the formation of Ag_2^+ clusters.

In the spectrum of Ag-NC100, the peaks at 325 and 290 nm were observed, attributed to Ag_8^0 and $Ag_8^{\delta+}$ clusters, respectively [25]. Such clusters have size larger than clinoptilolite channels diameters, but they were stabilized previously in mordenite channels (0.65×0.70 nm and 0.29×0.57 nm cross section) under similar conditions [25]. In addition, these peaks do not appear in the spectrum of Ag-SC100. Thus, we can suppose that large Ag_8^0 and $Ag_8^{\delta+}$ clusters are formed inside large mordenite channels, or in the interstitial spaces of the particles that compose this mineral.

The UV–vis DR spectra of the samples Ag-SC400 and Ag-NC400 (Fig. 4(b)) show a broad optical adsorption with asymmetric peaks centered at 300 and 410 nm due to surface plasmon resonance of silver nanoparticles. It shows that all four types of clusters (Ag_2, $Ag_4^{\delta+}$, Ag_8^0 and $Ag_8^{\delta+}$) are unstable after reduction at 400 °C.

The results concerning SAXS experiments are summarized in Table 1. The radius of gyration, within error range, remains constant and it corresponds to the inhomogeneous porosity of the samples. Likewise, fractal dimension values are not significantly altered by temperature or by silver impregnation. Radius of gyration and fractal dimension are the only precise parameters which can be determined by SAXS experiments without

Table 1
Gyration radius (Å) and fractal dimensions obtained by SAXS for all samples studied

Sample	Gyration radius (Å)	Fractal dimension
NC	180	1.88
Ag-NC100	172	1.88
Ag-NC400	174	1.82
Ag-NC500	173	1.82
SC	175	1.77
Ag-SC100	173	1.77
Ag-SC400	178	1.77
Ag-SC500	178	1.77

invoking supplementary hypothesis [35]. They are both mean parameters and correspond to the entire sample. Radius of gyration (the inertial distance from the gravity center) does not require any assumption on the shape of the scattering objects, hence it is a good parameter to estimate if the zeolite network is altered. In the same way, the fractal dimension is related to zeolite connectivity, thus if some extra-reticular alumina appear or if the zeolite network is locally destroyed the fractal dimension should diminish. Therefore, it seems from the SAXS results that the zeolite network is not altered with the silver exchange or the reduction process. The slight variations of the values reported in Table 1 do not allow us to make categorical conclusions about the stability of these materials with the increase of the reduction temperature. Mainly in the case of the natural clinoptilolite that, like we report previously, is a mixture of clinoptilolite, heulandite, mordenite and other mineral phases (quartz, feldspar, montmorillonite and iron oxides). The Kratky curves confirmed that all samples are similar and the scattering objects correspond to a globular shape since the curves present a broad peak.

In Fig. 5(b), the particle size distributions for Ag-SC100 and Ag-SC400 samples are presented. These distributions should correspond to the metal particles. As expected, the 400 and 500 °C samples presents larger particles (mainly radii of 5–15 nm) than the sample treated at 100 °C, which shows clearly resolved peaks for radius less than 10 nm, although most of the particles have 3, 5 and 6 nm.

The particle size distributions for samples Ag-NC100 and Ag-SC100 are similar (Fig. 5(a) and (b)), four sizes are defined and they are less than 7 nm. Observation of clusters inside clinoptilolite and mordenite pores with radius less than 0.2 and 0.35 nm is not possible by SAXS because the minimum radius limit of the technique is 0.5 nm. So SAXS (similar to XRD and TEM) is a technique that allows to study silver particles, but not silver clusters.

If particle size distributions for Ag-NC100, Ag-NC400 and Ag-NC600 samples are compared (Fig. 5(b)), the sintering of the metal particles is clearly appreciated. For Ag-NC100 sample, four sizes are defined and they are less than 7 nm. For Ag-NC400, the distribution turns out to be bimodal and the peaks are found at radii of 4 and 12 nm. The sample treated at 600 °C presents a very broad distribution, which includes particles with a radius of 16 nm. These results are in agreement with those obtained by XRD. For the observation of peaks of a compound, it is necessary that its amount be superior to 1%, and that the compound has to be crystalline and lastly the crystallite size has to be larger than 3 nm. Hence, the very small particles (less than 3 nm) are not detected by XRD but they may be registered by SAXS. Smaller clusters (<3 nm) can be registered by UV–Visible spectroscopy. The combination of XRD, SAXS and UV–Visible spectroscopy allows characterizing Ag particles in a wide size range. After reduction large particles on the surface of zeolite crystals are present, they are observed by XRD and SAXS but when clusters are formed they are only observed by UV–Visible spectroscopy.

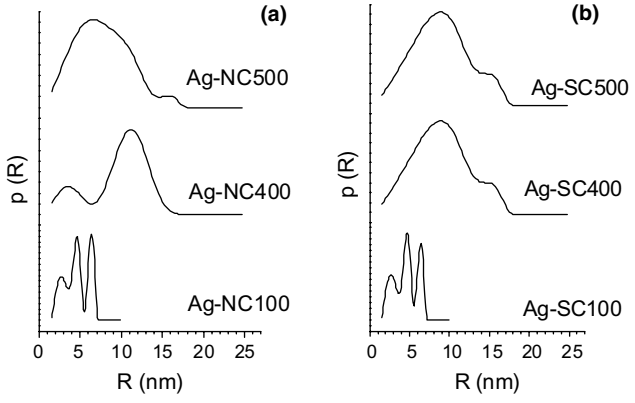

Fig. 5. Size distribution curves for: (a) Ag-NC100, Ag-NC400 and Ag-NC500 samples and (b) Ag-SC100, Ag-SC400 and Ag-SC500 samples obtained by SAXS.

4. Conclusions

The results obtained by the combined use of chemical analysis, XRD, UV–Visible spectroscopy and SAXS allowing to determine the state of silver in the zeolitic structure (natural and synthetic) and to study the particle size distribution of the Ag agglomerates present in the reduced samples.

The analysis of the UV–vis DR spectra of the samples reduced at 100 °C allows us to infer that in Ag-SC100 Ag_2^+ and $Ag_4^{\delta+}$ clusters stabilized inside clinoptilolite pores; while, in Ag-NC100 along with small Ag_2^+ and $Ag_4^{\delta+}$ clusters, large Ag_8^0 and $Ag_8^{\delta+}$ clusters are formed inside large mordenite channels or in the interstitial spaces of the particles that compose this mineral. Reduction at 400 °C leads to disappearance of silver clusters and large

particle formation. In both supports, the particles cannot be located in the zeolite cavities, which are much smaller.

The crystalline structure of the Ag-synthetic clinoptilolite (Ag-SC) was not affected by the thermal reduction of Ag, however, the Ag-natural clinoptilolite (Ag-NC) samples were less thermally stable. The existence of different exchangeable cations on NC in contrast to the high content of K^+ cation in SC which is responsible for this difference in thermal stability.

Acknowledgements

Authors thank Dr. A. Prakash for supplying synthetic clinoptilolite, Dr. V. Petravonskii for fruitful discussions, E. Flores, E. Aparicio, F. Ruiz, I. Gradilla and J. Diaz for technical assistance. This project is supported in part by the CONACYT, Mexico Grants No. E120.0862 and No. 42568-Q, Grant PAPIIT-UNAM IN109003 and by Havana University, ''Alma Mater'' research Grant No. AM907. B.C.R. is grateful to Y. Garcia for gently supplying Fig. 1; T. Farías and A. Pentón for their helpful comments. Mrs. M.C. Vela significantly improved the language of this manuscript.

References

[1] Ch. Baerlocher, W.H. Meier, D.H. Olson, Atlas of Zeolite Framework Types, Elsevier Science, New York, 2001.
[2] T. Armbruster, in: Proceedings of the13th International Zeolite Conference, Montpellier, France, Stud. Surf. Sci. Catal. 135 (2001) 13.
[3] B. Concepción-Rosabal, G. Rodríguez-Fuentes, R. Simón-Carballo, Zeolites 19 (1997) 47.
[4] G. Rodríguez-Fuentes, M.A. Barrios, A. Iraizoz, I. Perdomo, B. Cedré, Zeolites 19 (1997) 441.
[5] A. Lam, L.R. Sierra, G. Rojas, A. Rivera, G. Rodríguez-Fuentes, L.A. Montero, Micropor. Mesopor. Mater. 23 (1998) 247.
[6] A. Rivera, G. Rodríguez-Fuentes, E. Altshuler, Micropor. Mesopor. Mater. 24 (1998) 51.
[7] A.R. Ruiz-Salvador, D.W. Lewis, J. Rubayo-Soneira, G. Rodríguez-Fuentes, L.R. Sierra, C.R.A. Catlow, J. Phys. Chem. B 102 (1998) 8417.
[8] B. Concepción-Rosabal, J. Balmaceda-Era, G. Rodríguez-Fuentes, Micropor. Mesopor. Mater. 38 (2000) 161.
[9] M. Rivera-Garza, M.T. Olguin, I. García-Sosa, D. Alcántara, G. Rodríguez-Fuentes, Micropor. Mesopor. Mater. 39 (2000) 431.
[10] A. Rivera, G. Rodríguez-Fuentes, E. Altshuler, Micropor. Mesopor. Mater. 40 (2000) 173.
[11] A. Lam, A. Rivera, G. Rodríguez-Fuentes, Micropor. Mesopor. Mater. 49 (2001) 157.
[12] A.R. Ruiz-Salvador, A. Gómez, D.W. Lewis, C.R.A. Catlow, L.M. Rodríguez-Albelo, L. Montero, G. Rodríguez-Fuentes, Phys. Chem. Chem. Phys. (2000) 1803.
[13] D.W. Breck, Zeolite Molecular Sieves, Wiley, New York, 1974.
[14] K. Koyama, Y. Takeushi, Zeit. Kryst. 145 (1977) 216.
[15] M. Hotta, H. Nakajima, K. Yamamoto, M. Aono, J. Oral Rehabil. 25 (1998) 485.
[16] K.R. Bright, C.P. Gerba, P.A. Rusin, J. Hosp. Infect. 52 (2002) 307.
[17] ZZ: zeolite modified for the purification of water, National Institute of Hygiene of the Foods, Cuba, Sanitary Register No. 009/99–II/99, 1999, Cuba.
[18] Christopher C. Capelli, US Patent 5,607,683, March 4, 1997, US Patent 5,662,913, September 2, 1997.
[19] H. Shirakawa, O. Yamakawa, H. Nihonmatsu, K. Atsumi, US Patent 5,618,762, April 8, 1997.
[20] H. Illner, US Patent 5,709,672, January 20, 1998.
[21] N. Bogdanchicova, B. Concepción-Rosabal, N. Rubsov, T. Karamysheva, V. Gurin, M. Avalos-Borja, V. Petranoski, G. Rodríguez-Fuentes, ISSPIC 11 Proceedings, B-XVI-2, 2002.
[22] NRIB 1152: Quality requirements, Natural Zeolites for Pharmaceutical Industry, Drug Quality Control of Cuba, 1992.
[23] S.J. Chipera, J.A. Apps, in: D.L. Bish, D.W. Ming (Eds.), Natural Zeolites: Occurrence, Properties, Applications, Reviews in Mineralogy & Geochemistry, vol. 45, Mineralogical Society of America, Washinton, DC, USA, 2001.
[24] N. Bogdanchikova, E. Paukshtis, M. Dulin, V. Petranoskii, I. Shugi, T. Hanaoka, T. Matsuzaki, H. Tue, Sh. Shin, Inorg. Mater. 31 (1995) 451.
[25] N. Bogdanchikova, V. Petranovskii, R. Machorro, Y. Sugi, V.M. Soto, S. Fuentes, Appl. Surf. Sci. 150 (1999) 58.
[26] N. Bogdanchikova, V. Petranovskii, S. Fuentes, E. Paukshtis, Y. Sugi, A. Licea-Claverie, Mater. Sci. Eng. A 276 (2000) 236.
[27] N. Bogdanchikova, B. Concepción-Rosabal, V. Petranoskii, M. Avalos Borja, G. Rodríguez-Fuentes, Stud. Surf. Sci. Catal. 135 (2001) 243.
[28] O. Glatter, J. Appl. Crystallogr. 14 (1981) 101.
[29] O. Glatter, J. Appl. Crystallogr. 21 (1988) 886.
[30] O. Glatter, Prog. Colloid Polym. Sci. 84 (1991) 46.
[31] O. Glatter, B. Hainisch, J. Appl. Crystallogr. 17 (1984) 435.
[32] A. Guinier, G. Fournet, Small-Angle Scattering of X-rays, John Wiley & Sons Inc., New York, 1955.
[33] M. Kataoka, Y. Hagihara, K. Mihara, Y. Goto, J. Mol. Biol. 229 (1993) 591.
[34] M. Kataoka, J.M. Flanagan, F. Tokunaga, D.M. Engelman, Use of X-ray solution scattering for protein folding study, in: B. Chance et al. (Eds.), Synchrotron Radiation in the Biosciences, Clarendon Press, Oxford, 1994, p. 187.
[35] O. Glatter, K. Gruber, J. Appl. Crystallogr. 26 (1993) 512.
[36] A. Harrison, Fractals in Chemistry, Oxford University Press Inc., New York, 1995.
[37] J.E. Martin, A.J. Hurd, J. Appl. Crystallogr. 20 (1987) 61.
[38] V. Inglezakis, M. Loizidou, H. Grigoropoulou, J. Colloid Interface Sci. 275 (2004) 570.
[39] O.E. Petrov, in: D.W. Ming, F.A. Mumpton (Eds.), Natural Zeolites'93: Occurrence, Properties and Use, 1997, p. 271.
[40] I. Rodríguez-Iznaga, A. Gómez, G. Rodríguez-Fuentes, A. Benítez-Aguilar, J. Serrano-Ballan, Micropor. Mesopor. Mater. 53 (2002) 71.
[41] G. Gottardi, E. Galli, Natural Zeolites, Springer-Verlag, Berlin, Heidelberg, 1985, p. 409.
[42] A. Langella, M. Pansani, G. Cerri, P. Cappelletti, M. Gennaro, Clay Clay Miner. 51 (6) (2003) 625.
[43] L.L. Ames, Am. Mineral. 45 (1960) 689–700.
[44] P. Cappelletti, C. Colella, G. Cruciani, M. de'Gennaro, A. Langella, G. Oggiano, M. Pansini, in: C. Colella, F.A. Mumpton (Eds.), Natural Zeolites for the Third Millenium, De Frede, Naples, Italy, 2000, p. 151.